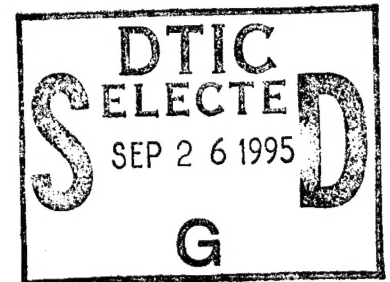OFFICE OF NAVAL RESEARCH

FINAL TECHNICAL REPORT

for

Contract N00014-91-J-1902

Project period: 01 July 1991-31 January 1992

Microwave Properties and Device Application of Ge_xSi_{1-x}/Si Superlattices

Kang L. Wang
University of California, Los Angeles
Electrical Engineering Department
405 Hilgard Avenue
Los Angeles, CA 90095-1594
Phone: (310) 206-7154

19950922 049

Final Technical Report

for

Microwave Properties and Device Application of Ge_xSi_{1-x}/Si Superlattices

N00014-91-J-1902

Project period: 07/01/91-01/31/92

This project entitled Microwave Properties and Device Application of Ge_xSi_{1-x}/Si Superlattices (N00014-91-J-1902)was a continuation of project entitled Fundamental Properties and Device Application of Ge_xSi_{1-x}/Si Superlattices (N00014-89-K-3227). Our investigation has been extended to expand the work in the study of Ge_xSi_{1-x}/Si superlattice and quantum well structures into the electromagnetic wave generation and detection applications. The study and its results for the additional 7-month period of experiment will briefly be discussed in the following. In this period, the energies of the minibands were investigated experimentally using the I-V-T measurement. The experimental values for the first and second miniband positions were 95 meV and 250 meV, respectively. These values were in good agreement with the calculated values of 91 meV and 220 meV from the emitter band edge taking the heavy and light-hole band splitting into consideration.

In addition, the I-V-T method was employed to determine the valence band discontinuity delta Ev in the coherently strained Ge_xSi_{1-x}/Si heterostructures. The results obtained were in good agreement with the theoretical calculations by pseudo potential method. The microwave time of flight set-up have been completed and microwave mobility measurement of the Si-Ge alloys was completed.

We investigated the quantum effects by fabricating resonant tunneling structures. Both light and heavy hole tunneling were observed in I(V), dI/dV characteristics. The tunneling species were identified by studying the magnetic field dependence of the tunneling peak positions. SiGe/Si superlattices were also been fabricated and the study of miniband transport was performed. The transport properties of minibands in SiGe/Si superlattices have been studied using both tunneling spectroscopy and thermionic analysis were in good agreement with the calculations using a transfer matrix technique including the light and heavy hole splitting. Resonant tunneling diodes with several different structure, grown at low temperature were studied by tunneling spectroscopy.

LIST OF RELATED PUBLICATIONS

1. R.P.G. Karunasiri, J.S. Park, Y.J. Mii and K.L. Wang, "Intersubband Absorption in $Si_{1-x}Ge_xSi$ Multiple Quantum Wells," Appl. Phys. Lett., 57 (24), 2585-2587, December 10, 1990.

2. S. Khorram, C.H. Chern and K.L. Wang, "Measurement of Valence Band Offset in Strtained Ge_xSi_{1-x}/Si Heterojunctions," the 14th International Symposium on Si-Based MBE, MRS, Anaheim, CA, Apr. 27-May 4, 1991.

MEASUREMENT OF VALENCE BAND OFFSET IN STRAINED Ge_xSi_{1-x}/Si HETEROJUNCTIONS

S. KHORRAM, C. H. CHERN AND K. L. WANG

Device Research Laboratory, 7619 Boelter Hall, University of California, Los Angeles, CA 90024

ABSTRACT

The valence band discontinuity ΔE_v in the coherently strained Ge_xSi_{1-x}/Si heterostructure is determined using I–V–T measurement. The electrical measurements of the band discontinuity of the pseudomorphic layers are difficult due to the thin layer imposed by the strain. Recently, low temperature growth of thick layer (>100 nm) of coherently strained Ge_xSi_{1-x} on Si has been achieved and thus made it possible for an accurate electrical measurement of band offset. The results obtained are in good agreement with the theoretical calculations by pseudopotential method.

INTRODUCTION

In recent years, Ge_xSi_{1-x}/Si heterostructures have been the subject of increasing theoretical and experimental interest. Strain induced band gap narrowing has been theoretically predicted by People [1], and experimentally demonstrated by Lang et al. [2]. In the Si–Ge heterosystem, strain effects add a new degree of freedom in design of novel band engineered heterostructures. Both the band gap and the band alignment are dependent on how each layer is strained. At the same time, due to critical thickness limitation on the coherently stained layer, it is difficult to make accurate measurement of important physical parameters such as mobility and band discontinuity. In this paper, we will discuss the measurement of valence band offset in Ge_xSi_{1-x}/Si heterostructure using thick, metastable, coherently strained Ge_xSi_{1-x} layers.

Early experimental observations by People et al. [3] had indicated that the major portion of band gap discontinuity in GeSi/Si system is in the valence band. This was later substantiated by the theoretical calculations of Van de Walle et al. [4] and People et al. [5]. There have been several attempts on experimental verification of band alignment using x– ray photoelectron spectroscopy (XPS) of Ge_xSi_{1-x}/Ge_ySi_{1-y} layers with different Ge compositions [6, 7, 8]. They reported large experimental error (> ±60 meV) associated with the XPS method.

Cap	Ge_xSi_{1-x}	$p = 5 \times 10^{17} \ cm^{-3}$
Barrier	Si	i
Buff	Si	$p = 5 \times 10^{17} \ cm^{-3}$
Sub	Si	p^+

Figure 1: Schematic diagram showing typical sample used to measure valence band offset.
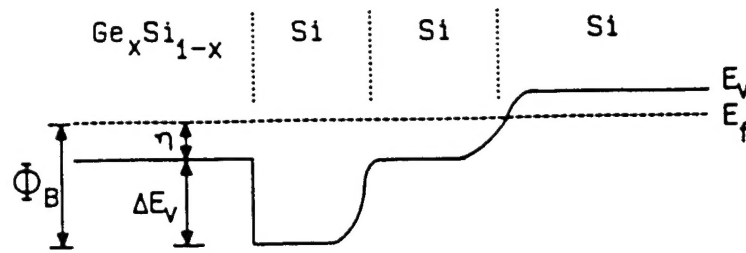
Figure 2: Band diagram for typical heterostructure used for I–V–T analysis.

In the present work, we have employed I–V–T measurement to investigate the valence band discontinuity in the strained Ge_xSi_{1-x}/Si heterosystem. This method has been used extensively to study the band alignment in AlGaAs/GaAs heterostructures [9, 10], which is a lattice matched system with no critical thickness limitation. In pseudomorphic heterostructures, such as in the Ge–Si heterosystem, this method can not be readily applied. Due to the lattice mismatch, at least one of the layers in Ge_xSi_{1-x}/Si heterostructures is strained. Moreover, only a limited thickness of a coherently strained layer can be grown. For example, if a coherently strained Ge_xSi_{1-x} layer is grown on a relaxed Si buffer layer, the Ge composition must be kept low for growth of a thick contact layer. On the other hand, if a strained silicon layer is grown on a relaxed Ge_xSi_{1-x} buffer layer, the barrier thickness must be kept small at high Ge compositons. However, when the barrier is thin, the tunneling through the barrier obscures the thermionic process at low temperatures.

In order to overcome the critical thickness problem, we have used a low temperature growth technique [11] to obtain metastable Ge_xSi_{1-x} layers with considerably larger pseudomorphic thickness than the conventional critical thickness. The structure as shown in Fig. 1 is designed such that the main component of the current is due to thermionic emission , and thereby the I–V–T method is fully exploited.

EXPERIMENTAL DETAIL

Figure 1 shows a schematic diagram of the typical sample structure used for the measurement. The samples used for this study were grown in a Si–MBE system on a p^+ Si substrate. Si wafers were chemically cleaned by Shiraki's method prior to loading in the system. Once inside the MBE chamber, the wafers were heated to 900 °C for desorption of the protective oxide layer. The substrate temperature was maintained at about 550 °C during the growth of the Si layer, and later it was reduced to 350 °C for the growth of the strained Ge_xSi_{1-x} layer. The structure consists of a 300 nm p-type Si buffer layer, followed by a 50 nm of an undoped Si layer, and capped by a thick p-type strained Ge_xSi_{1-x} layer. Depending on the Ge concentration, x, the thickness of the strained Ge_xSi_{1-x} layer was varied from 100–400 nm.

Table I. Sample structure and results.

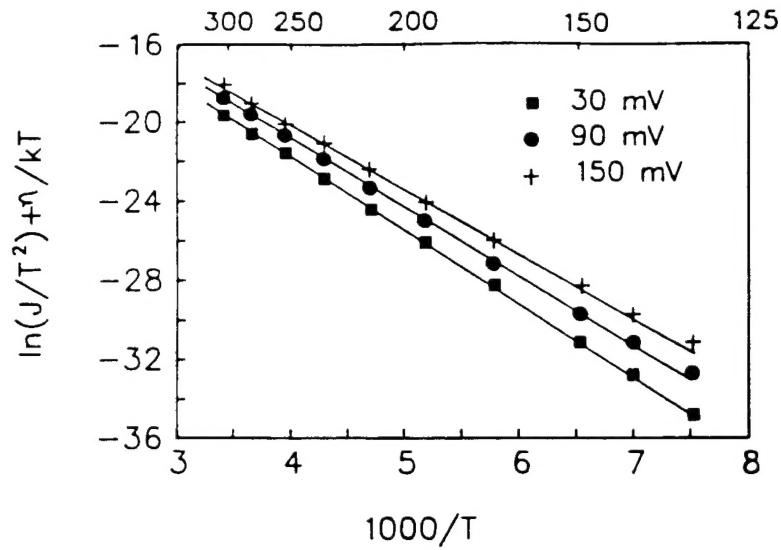| sample i.d.	Ge Mole fraction	Thickness Ge_xSi_{1-x} (Å)	Acceptor concentration (cm^{-3})	Measured ΔE_v (meV)	Theoretical calculation (meV)
CH162	0.3	3200	5×10^{17}	250±20	252
CH180	0.38	1500	5×10^{17}	330±20	320

Figure 3: Arrhenius plot of I–T data for several different bias points.

In order to avoid complications associated with the heavily doped semiconductors such as bandgap narrowing effect and strain relaxation, the layers were chosen to be lightly doped. The crystallinity and the quality of these layers has been verified by x–ray rocking technique and the Ge composition was checked by RBS.

The samples were processed using standard photolithography and lift–off procedures. Due to the metastability of the strained layers, high temperature alloying of ohmic contacts was avoided. The contacts were formed by evaporating Al and followed by annealing at 300 °C for 5 min. The top contacts which were circles of 25–100 microns in diameter were defined by a lift–off procedure. Device isolation was achieved by mesa etching down to the p^+ substrate. Several pieces of the processed sample were mounted on TO–5 headers and selected devices were wire–bonded for I–V–T measurement.

The I–V setup consists of a Keithley 602 electrometer, one Pd power supply model 2005, and two HP 3478A multimeters. Temperature control was accomplished with a resistive heater, a Harrison laboratories Inc model 6224A power supply, and L & N temperature controller. Temperature was measured by reading the voltage across a double junction J–type thermocouple wire. We were able to measure current levels down to 100 femto–Amperes, and the accuracy of our temperature reading was in the range of ±0.5 °C.

DATA ANALYSIS

The low voltage I–T data are analyzed based on the assumption that the current transport is governed by simple thermionic emission theory:

$$J = A^* T^2 exp\{\frac{-\Phi_B}{kT}\} \tag{1}$$

where

$$\Phi_B = \Delta E_v + \eta. \tag{2}$$

As Batey and Wright [12] have pointed out, in heterostructures Φ_B is from the top of the barrier to the Fermi level, as shown in Fig. 2. Moreover, the band offset can not be obtained by simply subtracting the ionization energy η, from Φ_B. We need to take into consideration the temperature dependence of the Fermi level in our data analysis. In the Ge–Si heterosystems, the ionization energy of dopant impurities such as boron varies from 10 meV to 45 meV, which may result in significant temperature dependence of the
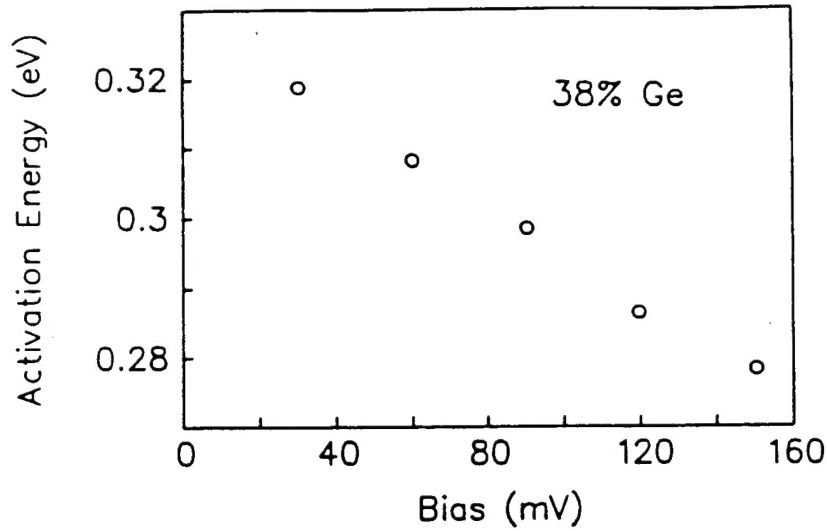
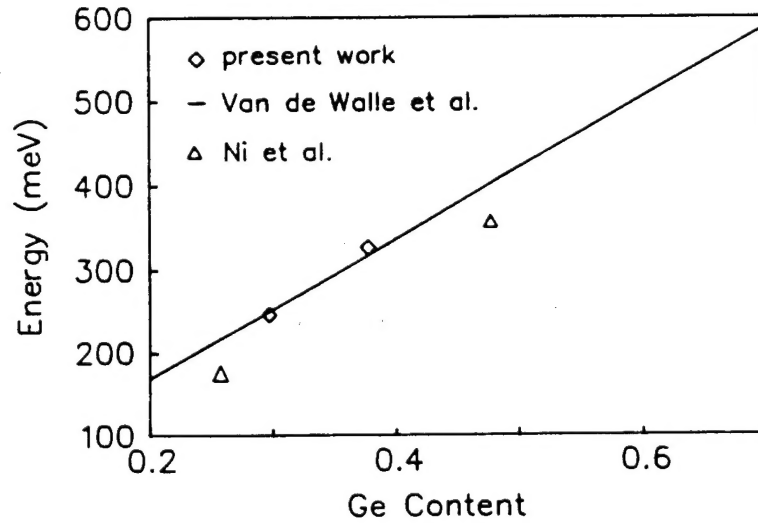Figure 4: Activation energy for the $Ge_{0.38}Si_{0.62}$/Si at different bias points.

Figure 5: Valence band alignment in strained Ge_xSi_{1-x} on Si substrate heterostructures.

Fermi level. For simplicity, we have assumed linear variation of ionization energy with germanium concentration, i.e.

$$E_i(x) = 10(meV) + x(45 - 10) \qquad (3)$$

where x is the germanium concentration in Ge_xSi_{1-x} alloy. The ionization energy obtained by this approximation has been used in the calculation of η, which has been incorporated in the data analysis.

The Arrhenius plot of I–V–T data of $Ge_{0.38}Si_{0.62}$/Si sample is shown in Fig. 3. Straight lines are plotted by the linear least- squares fitting method. The linear fitting shows a small standard deviation, ± 3 meV, which justifies the use of thermionic emission theory for data analysis.

The valence band offset is extracted from the extrapolation of the activation energy versus bias data, as shown in Fig. 4. At zero bias, we estimated the band bending close to hetero–interface is negligable. This might be a major source of error, which is included in the data uncertainty. We have designed all the semiconductor layers in and around the barrier with such a low level of doping that no significant band bending can occur (see

table I). The band offsets we obtained by I–V–T method are generally larger than the values reported by Ni et al. [6] using x–ray photoelectron spectroscopy (see Fig. 5). Our results are within 10% of pseudopotential calculations.

SUMMARY

The valence band discontinuity for strained layer Ge_xSi_{1-x}/Si was investigated using I–V–T method. The sample thicknesses and doping levels were designed to realize flat bands close to the heterointerface. The results obtained are in good agreement with pseudopotential calculations. Typical band offset measurement for $Ge_{0.38}Si_{0.62}/Si$ is about 330 meV. This implies that the Ge_xSi_{1-x}/Si heterosystems have high potential in band-engineered devices where a large band discontinuity is desirable.

References

[1] R. People. *Phys. Rev. B*, 32(2), 1405, 1985.

[2] D. V. Lang, R. People, J. C. Bean, and A. M. Sergent. *Appl. Phys. Lett.*, 47, 1333, 1985.

[3] R. People, J. C. Bean, and D. V. Lang. In *Proc. 1st Int. Symp. Silicon MBE, Pennington, NJ.*, page 364, 1985.

[4] C. G. Van de Walle and R. M. Martin. *Phys. Rev.*, B34, 5621, 1986.

[5] R. People, J. C. Bean, and D. V. Lang. *Proc. Inc. Conf. on Physics of Semiconductors*, 2, 767, 1986.

[6] W.-X. Ni, J. Knall, and G. V. Hansson. *Phys. Rev. B*, 36(14), 7744, 1987.

[7] G. P. Schwartz, M. S.Hybertsen, J. Bevk, R.G. Nuzzo, J. P. Mannaerts and G. J. Gualtieri. *Phys. Rev. B*, 39(2), 1235, 1989.

[8] E. T. Yu, E. T. Croke, T. C. McGill and R. H. Miles. *Appl. Phys. Lett.*, 56(6), 569, 1990.

[9] J. Batey, S. L. Wright, and D. J. DiMaria. *J. Appl. Phys.*, 57, 484, 1985.

[10] T. W. Hickmott and P. M. Solomon. *J. Appl. Phys.*, 57(8), 2844, 1985.

[11] C. H. Chern, K. L. Wang, M. A. Nicolet and G. Bai. to be published.

[12] J. Batey, and S. L. Wright. *J. Appl. Phys.*, 59, 200, 1986.

Intersubband absorption in $Si_{1-x}Ge_x$/Si multiple quantum wells

R. P. G. Karunasiri, J. S. Park, Y. J. Mii, and K. L. Wang

Device Research Laboratory, 7619 Boelter Hall, Department of Electrical Engineering,
University of California, Los Angeles, California 90024

The intersubband infrared absorption of holes in $Si_{1-x}Ge_x$/Si multiple quantum wells is observed. The quantum well structure consists of 10 periods of 40-Å-thick $Si_{0.6}Ge_{0.4}$ wells and 300-Å-thick Si barriers. The samples are prepared using molecular beam epitaxy. In the experiment, the infrared absorption as a function of wavelength is measured using a waveguide geometry. An absorption peak near 8.1 μm has been observed, which is due to the transition between first two heavy hole bound states. The polarization dependence spectra are in good agreement with the selection rules for the intersubband transition.

Intersubband absorption in quantum wells[1] and super-lattices[2] has attracted a great deal of attention due to potential application in infrared detection[3,4] and modulation.[5,6] Most of the studies have been performed using III-V based quantum wells and superlattices. Recently, infrared absorption between valence minibands of a $Si_{1-x}Ge_x$/Si superlattice at a fixed wavelength has been observed using photocurrent measurement.[7] In this letter, we report the first observation of intersubband infrared absorption in $Si_{1-x}Ge_x$/Si multiple quantum wells using Fourier transform infrared spectroscopy (FTIR).

The samples are grown in a molecular beam epitaxy (Si-MBE) system on high-resistivity (100 Ω cm) Si(100) wafers to reduce the infrared absorption due to free carriers in the substrate. The substrate is cleaned by a standard procedure[8] before it is loaded into the chamber and the protective oxide layer is removed by heating the substrate to 900 °C for 20 min. The substrate temperature is kept at about 540 °C during the growth of the quantum well structure.

In growth, first, an undoped Si buffer layer of 3000 Å thick is grown on the Si substrate. The multiple quantum well structure consists of 10 periods of 40-Å-thick $Si_{0.6}Ge_{0.4}$ wells and 300-Å-thick Si barriers. The center 30 Å region of the quantum wells is p doped to about 1×10^{19} cm^{-3}. The p-type doping is obtained using a thermal boron source.[9] The quantum well structure is capped with a 1000-Å-thick Si layer. The thick barrier layers keep the average Ge composition of the entire structure sufficiently low such that the total thickness of the $Si_{0.6}Ge_{0.4}$ layers is well above the critical thickness for a 40% Ge content. The schematic band structure of the sample used in the experiment is depicted in Fig. 1. In this figure, hole energy is taken to be positive for convenience.

The transmission spectrum of the sample is taken at room temperature using a Fourier transform infrared spectrometer. A waveguide structure of 5 mm long and 0.5 mm thick is prepared and employed (see inset of Fig. 2) for the measurement to enhance the absorption since the absorption strength is small due to the relatively large mass of the heavy hole ($0.26m_0$). A beam condenser is used to focus the infrared beam on the waveguide. An infrared polarizer is placed in the path of the infrared beam to probe the polarization dependence of the absorption process. In the case of intersubband transition, infrared absorption occurs only when the photon polarization has a nonzero component along the growth direction of the quantum well structure.[10]

The measured absorption spectrum as a function of wave number using the waveguide structure is shown in Fig. 2. The set of curves is due to the different polarization of the infrared beam and the zero degree corresponds to the polarization of the beam which is along the growth direction. A peak at 1230 cm^{-1} (8.1 μm) with a long tail towards the short wavelength region is observed. The small features superimposed on the spectra are mainly due to strong infrared absorption near 1100 cm^{-1} by SiO_2 and water bands in the spectral range of interest. The strength of the absorption decreases as the polarization of the infrared beam is rotated from the perpendicular direction towards the parallel direction of the plane of layers. Figure 3 illustrates the relative absorption strength as a function of the polarizer angle ϕ and the data follow the $\cos^2 \phi$ dependence (dashed curve) in agreement with the selection rule of the intersubband transition. The absorption strength (I_A) may be approximately estimated by the following expression:

$$I_A = \rho_s N_T \frac{e^2 h}{4c\epsilon_0 n_r m^*} f \frac{\cos^2 \theta}{\sin \theta} \cos^2 \phi, \quad (1)$$

where N_T is the total number of quantum wells that the infrared beam passes through due to multiple reflections, I_A is the integrated absorption strength, θ is the angle of
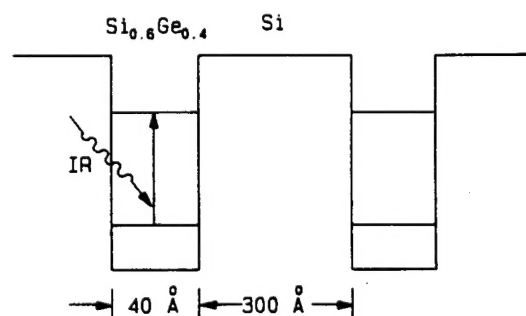

FIG. 1. Schematic band diagram of the multiple quantum well structure which consists of 10 periods of 40-Å-thick $Si_{0.6}Ge_{0.4}$ wells and 300-Å-thick Si barriers. The hole energy is taken to be positive.
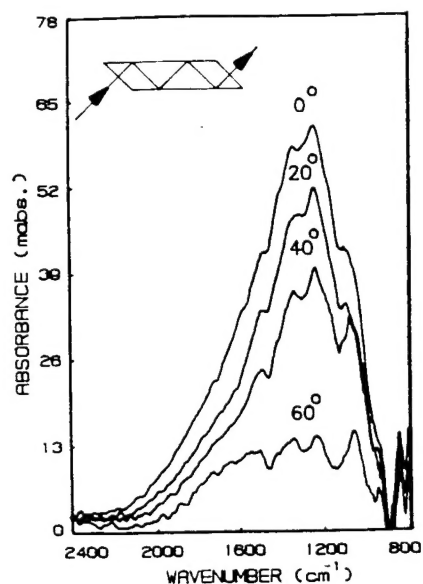
FIG. 2. Measured absorption spectra as a function of wave number for different polarization of the incident infrared beam. The peaks at 1230 cm^{-1} are due to intersubband absorption between the heavy hole ground and first excited states. The absorption strength at large polarization angles is shown to decrease in accordance with the selection rules of intersubband transition. The inset shows the waveguide structure used in the measurement.

incidence, ρ_s is the two-dimensional density of holes in the well, n_r is the refractive index, and m^* is the effective mass along (100) direction. Here, we ignore the nonparabolic effects on the intersubband transition both due to quantization and strain presence in the quantum well.

The oscillator strength of the transition (f) can be estimated using the above formula. For the structure we used $N_T = 100$, $m^* = 0.26m_0$, $n_r = 3.4$, $\theta = 45°$, $\rho_s = 3 \times 10^{12}$ cm^{-2} and the integrated absorption strength, $I_A = 40$ cm^{-1}. These parameters give the oscillator strength of 0.98 which is in good agreement with the values obtained for intersubband absorption in III-V based quantum well structures[1,3] which are in the 0.5–1.2 range. It should be
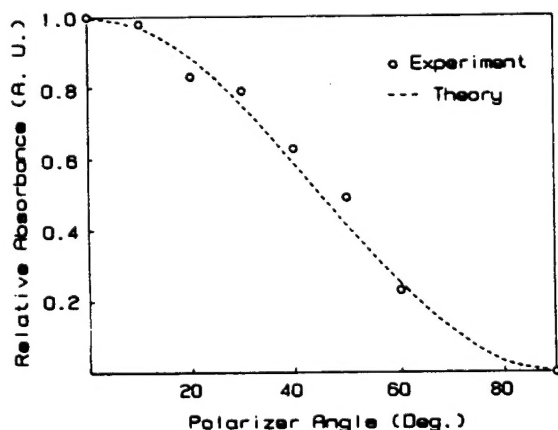

FIG. 3. Normalized absorption strength as a function of the polarization of the incident infrared beam. The zero degree corresponds to the polarization along the growth direction of the structure. The dashed curve shows the theoretically expected $\cos^2 \phi$ dependence.
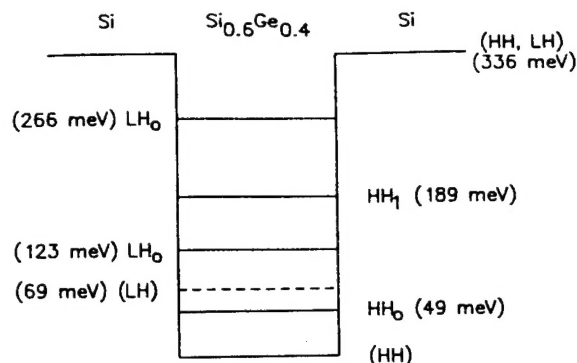

FIG. 4. Band structure of the Si/Si$_{0.6}$Ge$_{0.4}$/Si quantum well showing the bound states due to both light and heavy hole bands. The heavy hole (HH) and light hole (LH) band edges are shown in solid and broken lines, respectively.

cautioned that this is an approximate estimate as the nonparabolicity of the hole band can be severe in the quantum well and joint density of states effective mass can deviate significantly.[11]

The presence of three hole bands (heavy, light, and split-off) with energy separations close to the observed absorption peaks, makes the identification of the transitions not straightforward. However, the contribution from transitions between quantized states of two different hole bands is negligible due to the vanishing of matrix element of the transition.[12] This simplifies the deconvolution process. Figure 4 shows a detailed band diagram of the quantum wells due to the light and heavy hole bands along with the bound state energies. The bound state energies in the quantum well are calculated using envelope function approximation with the band offsets under compressive strain adopted from a linear interpolation of those of Van der Walle and Martin.[13] The effective masses of the light and heavy holes along (100) direction are obtained from Ref. 14, in which the effective masses are calculated using three band k·p and strain Hamiltonians.[15,16] The band offsets for the light and heavy holes are 267 and 336 meV and the effective masses are 0.22 and 0.26, respectively. There are two heavy hole bound states at 49 and 189 meV and two light hole states at 123 and 266 meV in the quantum well. All the energies are measured relative to the heavy hole band edge in the well region.

The light and heavy hole bands are degenerate in the Si barrier regions and are split in the well due to mass different quantization and the strain in the Si$_{0.6}$Ge$_{0.4}$ layer.[17] In the quantum well the light hole band lies about 70 meV above the heavy hole band while the split-off hole band is about 290 meV above the heavy hole band. These energy separations are relatively large compared with the kT at room temperature (~ 26 meV), and at thermal equilibrium most of the holes occupy in the heavy hole ground state. Thus, the intersubband absorption mainly occurs between quantized heavy hole states. The absorption peak at 1230 cm^{-1} (8.1 μm) is due to the transition between heavy ground state to the first excited state. The absorption peak width is about 600 cm^{-1} and is about a factor of 4 larger than intersubband absorption peak widths observed

in AlGaAs/GaAs quantum well structures.[1,3,18] This may be due to the strong nonparabolicity of the hole bands, in particular, in the presence of a strain. The calculated peak position for the transition between the ground and first excited heavy hole states is 140 meV and agrees reasonably well with the experimental value of about 153 meV. The structure used in this study is suitable only for absorption measurements since for the parameters used the first excited heavy hole state lies about 140 meV below the 300 Å Si barriers. However, for infrared detector application it is necessary to push the first excited heavy hole state close to the top of the barrier to efficiently collect the photoexcited carriers. This may be easily achieved by reducing the barrier height using a lower Ge composition in the quantum well.

In conclusion, we have observed the intersubband infrared absorption in $Si_{1-x}Ge_x/Si$ multiple quantum well structures. The nature of the optical transitions is characterized using the polarization dependence measurement and are in good agreement with the selection rules. The peak absorption strength is only a factor of 3, which is small compared to a similar structure used in the development of intersubband infrared detectors using AlGaAs/GaAs quantum wells. However, the possibility of increasing the doping density by at least an order of magnitude makes such structures useful for fabrication of Si-based tunable infrared detectors and modulators. Indeed, the monolithic integration of the GeSi/Si superlattice devices with Si integrated circuits may provide a new direction in optoelectronics.

[1] L. C. West and S. J. Eglash, Appl. Phys. Lett. 46, 1156 (1985).
[2] A. Kastalsky, T. Duffield, S. J. Allen, and J. Harbison, Appl. Phys. Lett. 52, 1320 (1988).
[3] B. F. Levine, R. J. Malik, J. Walker, K. K. Choi, C. G. Bethea, D. A. Kleinman, and J. M. Vandenberg, Appl. Phys. Lett. 50, 273 (1987).
[4] G. Hasnain, B. F. Levine, C. G. Bethea, R. A. Logan, J. Walker, and R. J. Malik, Appl. Phys. Lett. 54, 2515 (1989).
[5] Y. J. Mii, R. P. G. Karunasiri, K. L. Wang, M. Chen, and P. F. Yuh, Appl. Phys. Lett. 56, 1986 (1990).
[6] R. P. G. Karunasiri, Y. J. Mii, and K. L. Wang, Electron Device Lett. 11, 227 (1990).
[7] R. P. G. Karunasiri, J. S. Park, and K. L. Wang, Appl. Phys. Lett. 56, 1342 (1990).
[8] A. Ishizaka and Y. Shiraki, J. Electrochem. Soc. 133, 666 (1986).
[9] S. S. Rhee, R. P. G. Karunasiri, C. H. Chern, J. S. Park, and K. L. Wang. J. Vac. Sci. Technol. B 7, 327 (1989).
[10] D. D. Coon and R. P. G. Karunasiri, Appl. Phys. Lett. 45, 649 (1984).
[11] R. Wessel and M. Altarelli, Phys. Rev. B 40, 12457 (1989).
[12] E. O. Kane, J. Phys. Chem. Solids 1, 82 (1956).
[13] C. G. Van de Walle and R. Martin, J. Vac Sci. Technol. B 3, 1257 (1985).
[14] S. K. Chun and K. L. Wang, Effective Mass and Mobility of Holes in Strained $Si_{1-x}Ge_x$ Layers on (001) $Si_{1-y}Ge_y$ Substrate (to be published).
[15] G. E. Pikus and G. L. Bir, Sov. Phys. Solid State 1, 1502 (1960).
[16] J. C. Hensel and G. Feher, Phys. Rev. 129, 1041 (1963).
[17] R. People, Phys. Rev. B 32, 1405 (1985).
[18] Y. J. Mii, K. L. Wang, R. P. G. Karunasiri, and P. F. Yuh, Appl. Phys. Lett. 56, 1046 (1990).